FRACTURE STRENGTH OF THIN FILMS STUDIED BY INDENTATION TESTING

Akio Yonezu, Takeshi Ogawa and Mikio Takemoto

Department of Mechanical Engineering, Aoyama-Gakuin University
5-10-1, Fuchinobe, Sagamihara, Kanagawa, Japan

ABSTRACT

Using nano and micro indentation testing, we examined the effect of hard and soft substrates on the mechanical properties and strengths of thin films. Acoustic emission (AE) method was utilized to monitor micro cracks initiated during the indentation tests. We determined the critical indentation force, F_c, at the first film cracking by the AE method. The intrinsic properties of the thin film could be evaluated, when indentation force was below F_c value. Detected AE waveforms were analyzed using the polarity pattern in order to classify the cracking behavior. Fracture behavior of the thin film was studied from the viewpoint of the following results: relationship between force, F, and depth, h, (F-h curve), internal stress analyzed by the finite element method and observations of the contact region. It was revealed that bending stress was developed by indenter penetration and induced cracks for the soft substrate system. Using indentation testing, it is possible to estimate the bending strength of thin film.

Keywords Ceramic thin films, Indentation testing, Acoustic emission, Finite element method, Fracture strength

1. INTRODUCTION

Determination of the mechanical properties of thin films on substrates by indentation testing is always difficult because of the influence of the substrate on the measured properties [1]. Specifically, the property of a hard film/soft substrate system is difficult to measure, because the substrate is susceptible to deformation whereas hard substrates are not. The deformation of substrates may induce film cracking. Therefore, we should perform indentation testing below the force, at which the film cracking occurs. In order to measure the intrinsic properties of thin films, the common rule limits the indentation depth less than 10% of the film thickness [2]. However, the precise measurement of the indentation response is difficult for very thin films because of environmental anomalies such as temperature fluctuation, airflow and small vibration. Although researchers have used both experimental and theoretical methods to study the problem [3][4], the film properties could not be measured when film cracking occurred. However, there is a possibility to evaluate the mechanical properties and the fracture strength for the thin film by a study of the mechanism of film cracking with the substrate deformation.

In this study, we performed indentation testing for ceramic thin film to study the influence of the substrate material. During indentation testing, acoustic emission (AE) method was used to study the behavior of thin film cracking and determine indentation force at which the film cracking occurred. We also evaluated the fracture strength of thin film using the finite element method (FEM).

2. MATERIALS AND EXPERIMENTAL PROCEDURES

The materials used for this study were ceramic TiN thin films. The TiN coating was deposited by sputtering onto two substrates, i.e. stainless steel (SUS304) and tungsten carbide cermet

Table 1 Materials and specimen size.

Material	TiN/SUS304	TiN/WC-Co
Substrate	SUS304	WC-Co
Film thickness (μm)	4	2
Specimen size (mm)	20 x 20 x 2	20 x 20 x 5

(WC-Co). Film thickness and specimen size are shown in Table 1.

Several instruments for indentation testing were used to perform the tests with a wide range of indentation force between 5 mN and 10 N. We evaluated the hardness of both the film coated specimens and substrate specimens using Scanning Piezoelectronic Hardness Tester (SPH-1), DUH-201 (Dynamic Ultra Micro Hardness Tester), and HMV-2000 (Hardness Micro Vickers Tester) of SIMADZU Co.. The sustained loading time, t_v, was 5 s, and the loading and unloading rates, dF/ds, was 0.237～23.54 mN/s. We repeated the tests five times in each condition and averaged the results. For the SPH-1 and DUH-201 with Berkovich indenter tip, the hardness values were calculated from F-h curves, however for HMV-200 with Vickers indenter, they were calculated from the measurement of the diagonal lines of the indentation damage.

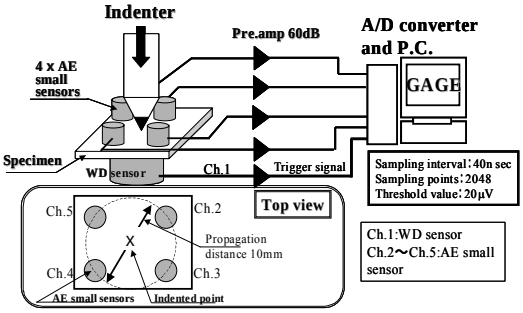

Fig.1 Experimental setup for AE system for indentation testing.

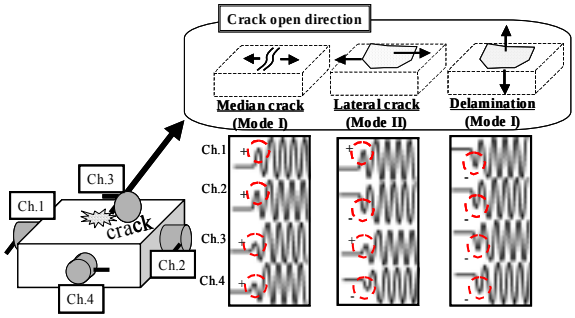

Fig.2 The schematics of elastic waveforms due to three types of cracking during indentation tests.

We performed micro indentation testing with an electro magnetic type servo-testing machine equipped with a Vickers indenter and two eddy current sensors. It can measure F-h curve with high resolution and vary the loading conditions, i.e. dF/ds, load holding value (maximum indentation force), F_{max}, and holding time, t_v. All tests were performed with constant value of dF/ds = 5 mN/s and t_v =10 s at room temperature.

We monitored AEs using four resonant type small sensors (PAC, Type PICO), which were mounted on the top surface of the specimen, and used a wide band frequency sensor (WD: PAC), which was mounted on the backside of the specimen, as shown in Fig. 1. The WD sensor signal was set on the trigger channel. As shown in this figure, the AE system consists of four small sensors and WD sensor with 60 dB preamplifiers (PAC), an A/D converter (GAGE applied Inc.) and a personal computer. We monitored AEs by recording data from 2048 points with an interval of 40 ns. The threshold value for channel 1 (trigger channel) was set at 20 μV.

AE characteristics or fracture types during indentation tests were classified using the radiation pattern of waveforms [5], as illustrated in Fig.2. The median crack, which is a Mode I crack, generates AE waveforms whose first peaks have all positive polarities. Lateral crack, which is a Mode II (in-plane sliding) crack, grows parallel to the specimen surface. On the opposite sides of the specimen, the first polarities of the waveforms are anti-symmetric. The delamination, which is a Mode I fracture, produces a crack opening parallel to the surface, and the polarities of the first peaks are all negative.

3. RESULTS AND DISCUSSION

3.1 Hardness testing

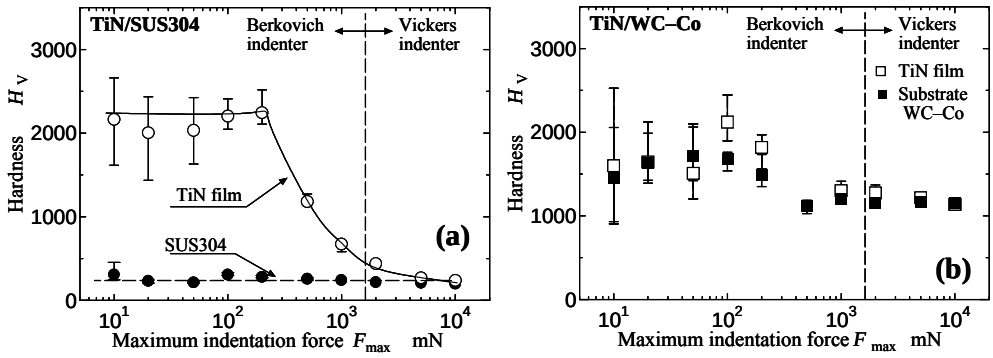

Fig.3 Hardness for TiN/ SUS304 (a) and TiN/WC-Co (b).

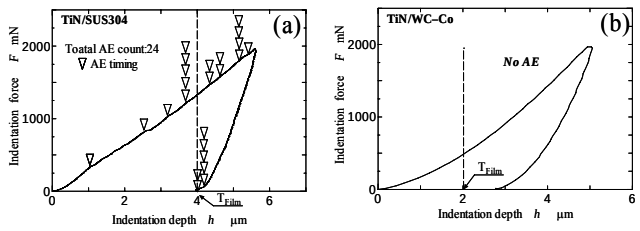

Fig.4 *F- h* curve with AE timing for TiN/SUS304 (a) and TiN/WC-Co (b).

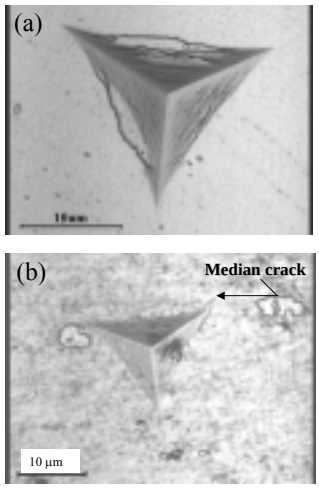

Fig.5 Micrographs of contact region for TiN/SUS304 (a) and TiN/WC-Co (b), tested with F_{max}=2N using Berkovich indenter.

Figure 3 shows the variation of Vickers hardness, *HV*, as a function of F_{max}. The *HV* value was calculated using following equation [6], which compensates the indentation size effect.

$$HV=[F/\{4.6248\text{x}10^{-4}(h+40.468)^2\}]^{1.023} \quad (1)$$

where F and h are substituted for F_{max} and the plastic indentation depth obtained from the unloading portion of *F-h* curve, respectively. In Fig.3, open marks represent the hardness of film, HV_{Film}, and solid marks represent the hardness of substrates, HV_{sub}. As shown in Fig.3 (a) (TiN/SUS304), the HV_{Film} became similar to the HV_{sub} when F_{max} >10 N, while it gradually increased with decreasing of F_{max}. Below the F_{max} of 200 mN, the HV_{Film} gave a constant value. This result suggested that the intrinsic HV_{Film} could be obtained for F_{max} < 200 mN. In Fig.3 (b) (TiN/WC-Co), both HV_{Film} and HV_{sub} have large scatter under low indentation force, but overall HV_{Film} values are quite similar to the HV_{sub} value independent of F_{max}. However, HV_{Film} values indicated smaller than those of TiN/SUS304. This difference might be attribute to small difference of coating conditions, since those specimens were treated by different companies.

3.2 Analysis of micro crack behavior using AE method

The AE method was used to study micro cracking behavior. We determined the critical indentation force, F_c, at the on set of film crack using the DUH. The F_{max} for these tests were 2 N. Figure 4 shows the *F-h* curves together with the AEs detected points, shown by ▽ marks. In Fig.4 (a), we detected 24 AEs during the test. 17 of these were found during the loading process. The first AE may correspond to the initial film cracking. The value of F_c was around F=300 mN.

Subsequent AEs caused the fluctuation of the *F-h* curve. Figure 5 shows micrographs of the contact region of the above tests. In TiN/SUS304, film cracks appeared and rippled out from the contact region. These cracks may have generated AEs during the loading process, as shown in Fig.4 (a). In TiN/WC-Co, cracking behavior was remarkably different from that of TiN/SUS304. Small median cracks originated from the corners of the contact region. Under indentation testing, this behavior is similar to that of monolithic ceramics. We could not detect any AEs during this test as shown in Fig.4 (b), because the sizes of these median cracks were too small to generate detectable AEs with our system.

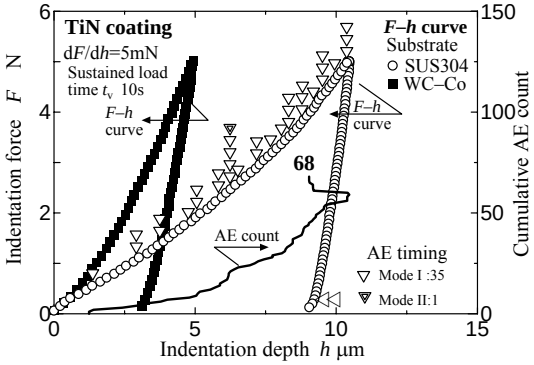

Fig.6 *F-h* curve with cumulative AE count for TiN/SUS304 and TiN/WC-Co.

We performed the micro indentation tests at F_{max} = 5 N using an electro magnetic servo-testing machine equipped with a Vickers indenter. Figure 6 shows the *F-h* curves and cumulative AE counts. The result for TiN/SUS304 shows many AEs especially during the loading process, while no AEs could be detected in TiN/WC-Co. Based on the fracture type classification method [6] as demonstrated in Fig.2, we analyzed monitored AE waveforms during the indentation test for TiN/SUS304. In figure 6, the shape of triangle marks indicate the fracture types estimated by the AE analysis. We detected many Mode I AEs during the loading process. This behavior revealed that these types of AEs were generated from Mode I crack, which opened perpendicular to the specimen surface.

Figure 7 shows the micrographs of contact region after the tests. In TiN/SUS304, many film cracks appeared, and rippled out from the contact region extensively. This type of crack may eradiate the AEs during the loading process. It is assumed that this crack initiates at a certain distance due to the film bending upon indenter penetration. However, in TiN/WC-Co, small median cracks originated from the corners of indentation damage, which was similar to Fig.5 (b).

We measured the spacing of the rippled cracks in TiN/SUS304 in order to evaluate the fracture strength of thin film. Figure 8 shows the number of cracks found in the contact region as a function of distance from the center of indent, *r*. The crack number is started to count when the *r* value is more than half of the coating thickness. Solid marks indicate the data achieved from the indented area after the indenter reached the substrate. The lines on the graph are expressed in liner-regression lines for the open and solid marks. The reciprocal of the slope in these lines is the spacing of the rippled cracks, L_c, which initially increase with

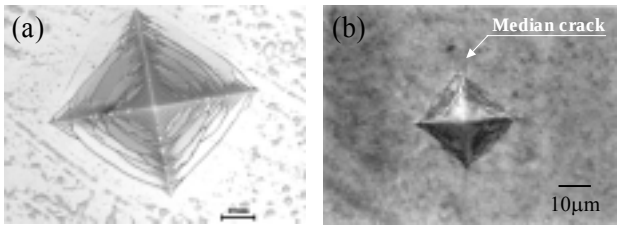

Fig.7 Micrographs of contact region for TiN/SUS304 (a) and TiN/WC-Co (b), tested with F_{max}=5N using Vickers indenter.

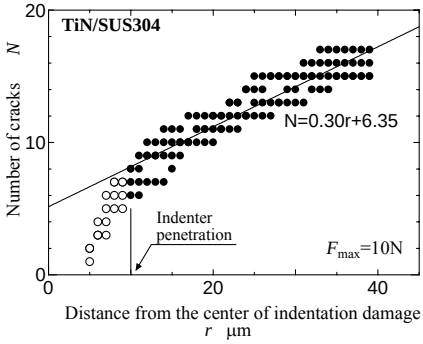

Fig.8 Number of cracks as a function of the distance from the center of contact region.

increasing r and become constant, when r is larger than the coating thickness. We prepared additional specimen with film thickness, t_F, of 2 μm by grinding off the film, and performed tests with F_{max} of 5, 10 and 20 N in both t_F=2 μm and 4 μm specimens. Figure 9 shows the constant L_c, obtained from similar plots with Fig.8 for different coating thickness and F_{max} values. As a result of these tests, the L_c is independent of F_{max}. The L_c values for t_F=4 and t_F=2 μm were 3.7 and 2.3 μm, respectively. It was found that the thinner the film, the smaller the spacing of cracks.

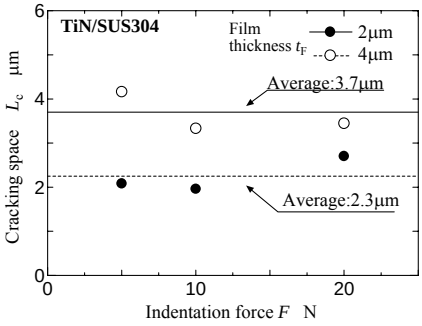

Fig.9 Cracking space, L_c, against with indentation force.

3.3 Evaluation of fracture strength

We used the finite element method (FEM) in order to study the influence of the substrate on internal stress of the thin film. Two structural models were created for TiN/SUS304 and TiN/WC-Co. The film thickness of the models was 4 μm. The yield stress, σ_{ys}, of the film assumed to be 7 GPa estimated by three times of *HV* value [7]. Figure 10 shows stress σ_x distribution for the direction parallel to the specimen surface on the free surface for h of 2 to 10 μm, where the horizontal axis, r, is originated from the center of contact region. The △ marks indicate the boundary of contact region between the coating surface and the indenter. In Fig.10 (a), the σ_x is compressive in the contact region. However, the σ_x appeared to be tensile outside of the contact region, because the bending stress of thin film caused by the indenter penetration developed outside the point of contact. As a result, film cracking due to film bending took place in the soft substrate as explained in section 3.2. When the bending stress reaches the fracture strength of the thin film, rippled crack is formed. The cracking releases the bending stress, which increases again at the neighboring film surface under the subsequent indentation. On the contrary, only the compressive value of σ_x appeared for TiN/WC-Co, as demonstrated in Fig.10 (b). In this case, the substrate was not susceptible to deformation, compared with TiN/SUS304. Therefore, the crack type in hard substrate is similar to that of monolithic ceramics, as shown in Fig.5 (b) and 7 (b).

We studied the fracture strength of thin film for both specimens with t_F of 2 and 4 μm specimens using the similar FEM model above. We created simulated cracks at r=25 and 15 μm for the models of t_F =4 μm and 2 μm specimens, respectively. When the film cracking occur, σ_x in the film is released. However, further indentation increased σ_x again.

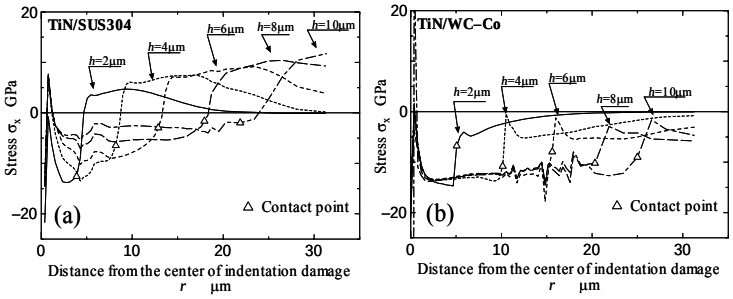

Fig.10 σ_x distribution for TiN/SUS304 (a) and TiN/WC-Co (b).

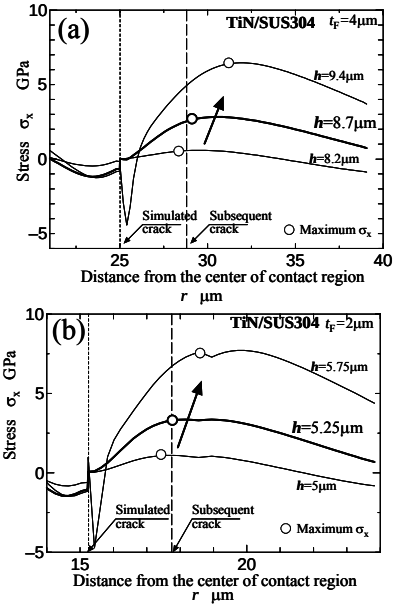

Fig.11 σ_x distribution for TiN/SUS304 with t_f=4 μm(a) and 2 μm(b).

When σ_x achieved the fracture strength of film, the next film crack developed. Figure 11 shows the σ_x distribution on the subsurface of the specimen. The depth is 1/10 of film thickness, because the stress concentration took place near the edge of simulated crack on the specimen surface. In this figure, the dotted line indicates the position of the simulated crack, and the dashed line indicates that of the next cracking, which was estimated by the results in Fig.11 (i.e. 2.3 μm and 3.7 μm for t_F=2 μm and 4 μm specimens, respectively). As shown in these figures, it was found that σ_x released at the position of the simulated crack. We also found that the value of the maximum σ_x increased and its position shifted with increasing h. When the maximum σ_x value is achieved at the position of the next crack, this value can be regarded as the fracture strength of the thin film. These values were 2.9 and 3.3 GPa for t_F of 4 and 2μm, respectively. The estimated values of σ_x were approximately the same independent of the film thickness. The averaged value was 3.1 GPa. It should be noted that the true values include the effect of residual stress of thin films, which has been reported to be 3.5 GPa in compression.

4.CONCLUSION

Using indentation testing, we examined the effect of hard and soft substrates on the mechanical properties, fracture behavior and strengths of thin films. The results are summarized as follows.

1. With wide range of indentation forces between 5 mN and 10 N, indentation tests were performed for TiN coated materials with soft (SUS304) and hard (WC-Co) substrate. For TiN/WC-Co, overall the *HV* of the film are quite similar to that of substrate and independent of indentation force. While, for TiN/SUS304, the *HV* of the film gradually increased with decreasing indentation force and gave a constant value, which is the intrinsic *HV* of the TiN film. Using AE method, we detected the first film cracking in TiN/SUS304 during the test. We found that the mechanical properties of the thin film could be evaluated, prior to the initiation of film cracking.
2. In TiN/WC-Co, median cracks initiated at the corners of contact region, similar to monolithic ceramics. While in TiN/SUS304, many film cracks appeared and rippled out from the damaged area. Using AE analysis, these crack initiations were found to be Mode I cracking, which opened perpendicular to the specimen surface.
3. Only for soft substrate, it was found that the film cracking occurred due to the supple nature of the substrate and the consequent bending of the film. By measuring the spacing of film cracks and their FEM simulations, we calculated the fracture strength of the film. The value of TiN thin film was 3.1 GPa, independent of the film thickness.

ACKNOWLEDGEMENT

This work was performed as a part of the Center of Excellence (COE) Program, funded by the Ministry of Education, Culture, Sports, Science and Technology.

REFERENCES

(1)R.Saha, W.D.Nix; Acta Materialia, **50**,23-38, (2002). **(2)**W.C.Oliver, G.M.Pharr; Journal of Material research, **7**,6,1564- 1583, (1992). **(3)**T.Y. Tsui, G.M.Pharr; Journal of Material research, **14**,1,292- 301, (1999). **(4)**Y-T,Cheng, C-M,Cheng; Applied Physics Letter, **73**,5,614-616 (1998). **(5)**A. Yonezu, T. Ogawa and M. Takemoto; Progress in Acoustic Emission **XI**, 86-93, (2002). **(6)**K.Miyahara, N.Nagashima, S.Matsuoka, T.Ohmura; Journal of the Japan Society of Mechanical Engineering, **64**,626,2567-2673 (1998) in Japanese. **(7)**D.Tabor; *The Hardness of Metals*, Oxford university press, **1**-1541951). **(8)**S.Ogawa, T.Fukai, T.Futatsugi, M.Takemoto; Surface technology, **46**,5,456-463, (1995), in Japanese. **(9)**K.Suzuki, H.Matubara, A.Matuo, K.Shibuki; Journal of the Japan Institute of Metals, **49**,773, (1985) in Japanese.